MINISTRY OF EDUCATION AND TRAINING

VIET NAM ACADEMY OF SCIENCE AND TECHNOLOGY

GRADUATE UNIVERSITY OF SCIENCE AND TECHNOLOGY

PHAM MINH THUY

RESEARCH ON FABRICATION OF PHOTOCATALYTIC MATERIALS BASED ON TiO_2 AND ZnO MODIFIED BY NITROGEN-DOPED GRAPHENE QUANTUM DOTS AND SILVER NANOPARTICLES

SUMMARY OF DISSERTATION ON MATERIALS SCIENCE

Major: Theoretical and Physical Chemistry

Code: 9 44 01 19

The dissertation was completed at: Graduate University of Science and Technology, Vietnam Academy Science and Technology

Supervisors:

1. Supervisor 1: Assoc. Prof. Vu Duc Chinh, Institute of Institute of Materials Science, Vietnam Academy of Science and Technology

2. Supervisor 2: Dr. Chu Thi Thu Hien, Hanoi university of Civil Engineering

Refferee 1:.....

Refferee 2:.....

Refferee 3:.....

The dissertation is examined by Examination Board of Graduate University of Science and Technology, Vietnam Academy of Science and Technology at …….. (time, date, year…)

The dissertation can be found at:

1. Graduate University of Science and Technology Library
2. National Library of Viet Nam

INTRODUCTION

The urgency of the thesis

Aquatic pollution caused by toxic organic substances in Vietnam, which are difficult to decompose, has been a rising problem in recent years. Combining noble metals and carbon nanomaterials with traditional photocatalysts can increase the decomposing yield of pollutants and enlarge the light absorption band. Therefore, natural sunlight can indeed be utilized to activate these materials, reducing the time and operating costs associated with the pollution treatment process.

Research objectives

- Synthesis of nitrogen-doped graphene quantum dots and silver nanoparticles modified TiO_2 and ZnO.

- Evaluate the photocatalytic activity of synthetic materials for methylene blue degradation in aquatic environments under light irradiation.

Research contents.

+ Research on the fabrication of titanium dioxide (TiO_2) and zinc oxide (ZnO) materials.

+ This research focuses on the fabrication of TiO_2 and ZnO materials that have been modified with silver (Ag) nanoparticles.

+ Research on the fabrication of TiO_2 and ZnO modified by nitrogen-doped graphene quantum dots (N-GQDs).

+ Research on the simultaneous fabrication of TiO_2 and ZnO materials modified with nitrogen-doped graphene quantum dots (N-GQDs) and Ag nanoparticles.

+ Investigate the characteristic physicochemical properties of the materials that have been fabricated.

+ An investigation and comparison of the photocatalytic capabilities of the synthesized materials.

Scientific and practical basis of the topic

Scientific basis

To enhance the catalytic ability of TiO_2 and ZnO materials, the thesis aims to combine them with the effects of carbon and precious metal. This involves developing the fabrication techniques for carbon and precious metal nanomaterials and studying their structures, optical properties, and the photocatalytic enhancement effects.

Practical basis

The thesis presents initial experimental solutions and applications for the photocatalytic material systems Ag, N-GQDs/TiO_2 and Ag, N-GQDs/ZnO, aimed at decomposing well-dispersed organic compounds in an aqueous environment.

New contributions of the thesis

Science and Technology:

- The establishment of an environmentally friendly fabrication process for two new multilayer photocatalytic materials that effectively operate in the visible spectrum: Ag, N-GQDs/TiO_2 and Ag, N-GQDs/ZnO.

- An analysis of the optimal content ratio of nano silver (Ag) and nitrogen-doped graphene quantum dots (N-GQDs) that can be effectively modified on the surfaces of the traditional photocatalysts, titanium dioxide (TiO_2) and zinc oxide (ZnO).

- A proposal of a chemical structure model for N-GQDs, along with diagrams illustrating the reduction of Ag^+ ions to Ag by N-GQDs and charge transport in Ag, N-GQDs/TiO_2.

- A detailed outline of the processes involved in the emission and non-emission relaxation of electron-hole pairs in Ag/TiO_2 nanoparticles, including an analysis of the kinetics and insights into the decay processes.

Application:

A viable technological solution for caffeine treatment has been proposed.

CHAPTER 1. LITERATURE REVIEW

1.1. Overview of Photocatalytic Materials

1.1.1. Mechanism of Photocatalytic Reactions

1.1.2. Factors Affecting Photocatalytic Activity

1.1.3. Titanium Dioxide (TiO_2)

1.1.4. Zinc Oxide (ZnO)

1.2. Noble Metals

1.2.1. Mechanism of Charge Transport

1.2.2. Mechanism of Local Electric Field Enhancement

1.3. Graphene and Graphene Quantum Dots

1.3.1. Graphene

1.3.2. Graphene Quantum Dots

1.3.3. Mechanism of Enhanced Photocatalytic Efficiency in Graphene Materials

1.4. Current Research on Graphene and Noble Metals in Photocatalysis

1.5. Conclusion

CHAPTER 2. OBJECTS AND RESEARCH METHODOLOGY

2.1. Research Objects

2.2. Research Methods

2.2.1. Synthesis Methods

2.2.1.2. Fabrication of N-doped graphene quantum dots and Ag nanoparticles modified TiO_2

a. TiO_2

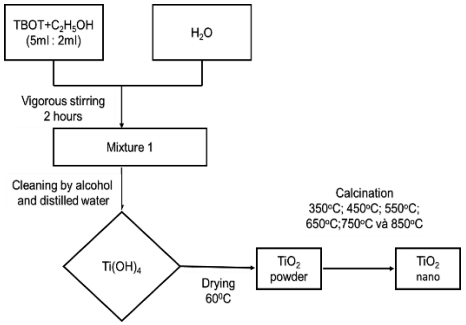

Fig 2.1. The schematic diagram of the synthesis of TiO_2

b. Ag modified TiO_2

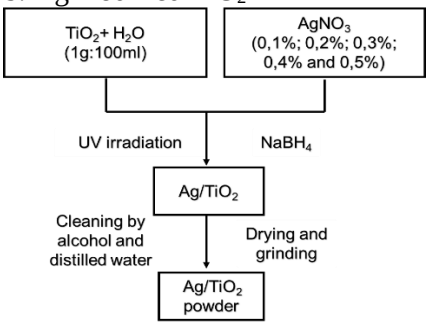

Fig 2.2. The schematic diagram of the synthesis of Ag/TiO_2

c. N-GQDs modified TiO_2

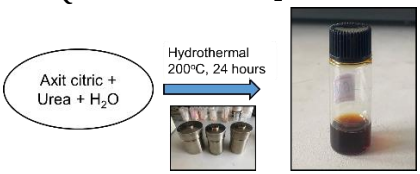

Fig 2.3. The schematic diagram of the synthesis of N-GQDs

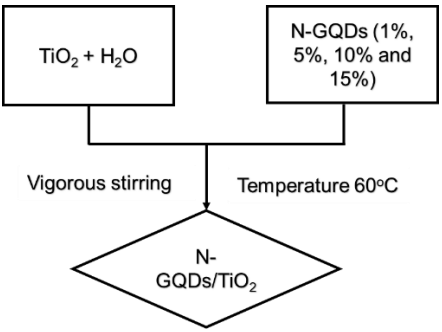

Fig 2.4 The schematic diagram of the synthesis of N-GQDs/TiO_2

d. Ag, N-GQDs modified TiO_2

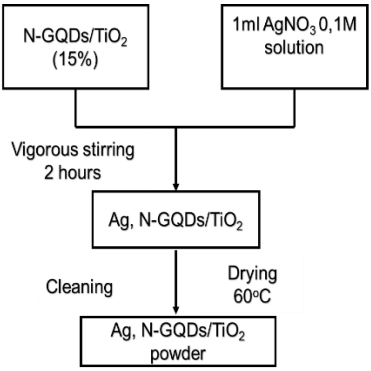

Fig 2.5. Schematic diagram for the fabrication of Ag, N-GQDs/TiO_2

2.2.1.3. Fabrication of N-doped graphene quantum dots and Ag modified ZnO

a. ZnO

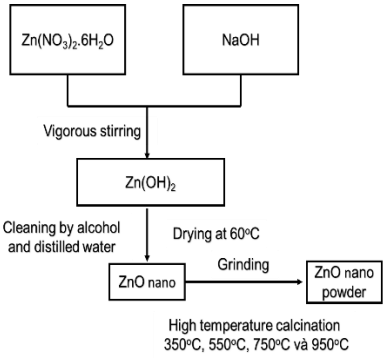

Figure 2.6. The schematic diagram of the synthesis of ZnO

b. Ag modified ZnO

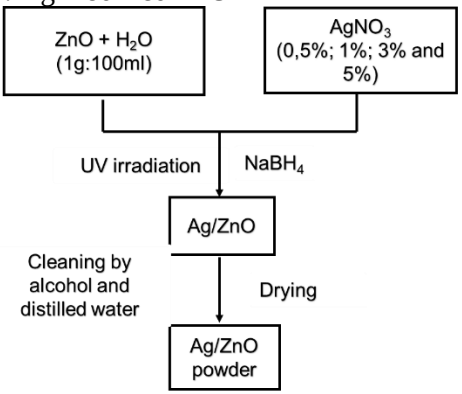

Figure 2.7. The schematic diagram of the synthesis of Ag/ZnO

c. N-GQDs modified ZnO

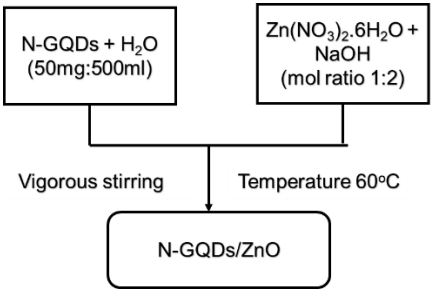

Figure 2.8. The schematic diagram of the synthesis of N-GQDs/ZnO

d. Ag, N-GQDs modified ZnO

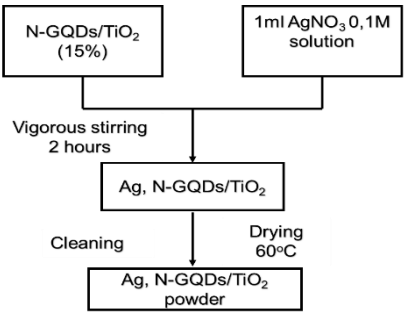

Figure 2.9. The schematic diagram of synthesis of Ag, N-GQDs/ZnO

2.2.2. Methods for Studying the Morphology and Structure of Materials

2.2.2.1. X-ray Diffraction

2.2.2.2. Scanning Electron Microscopy SEM

2.2.2.3. High-Resolution Transmission Electron Microscopy HRTEM

2.2.2.4. Fourier Transform Infrared Spectroscopy

2.2.2.5. X-ray Energy Dispersive Spectroscopy

2.2.2.6. X-Ray Photoelectron Spectroscopy

2.2.2.7. PL Fluorescence Spectroscopy

2.2.2.8. Raman Spectroscopy

2.2.2.9. UV-Vis Absorption Spectroscopy

2.2.3. Methods for Studying the Photocatalytic Activity of Materials

CHAPTER 3. RESEARCH RESULTS

3.1. Research results on the characteristics and photocatalytic activity of nitrogen-doped graphene quantum dots and silver-modified TiO_2.

3.1.1. Titanium Dioxide

3.1.1.1. Characteristics of TiO_2

a) X-ray diffraction pattern of TiO_2

When the calcination temperature ranges from 350°C to 850°C, a phase transition of TiO_2 occurs. The form in which TiO_2 exists is temperature-

dependent; the anatase phase is present at temperatures below 650°C, while the rutile phase appears at temperatures above 650°C. This phase transition of TiO_2 is an irreversible process, and the crystal size of TiO_2 increases from 16 nm to 40 nm as the temperature rises.

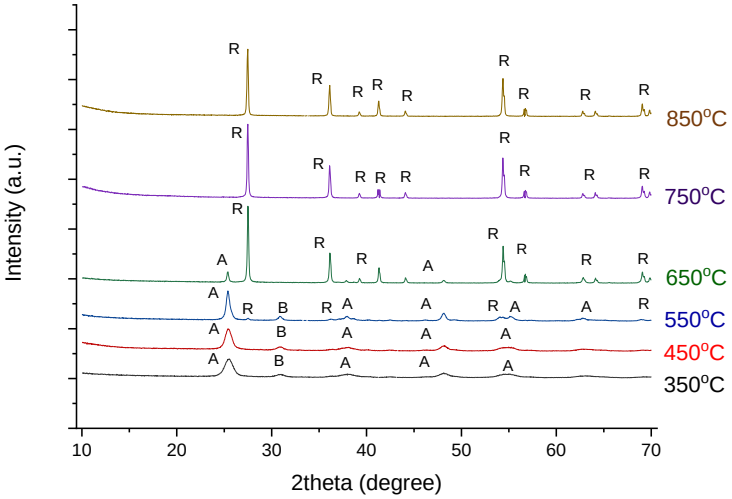

Figure 3.1. XRD pattern of TiO_2 synthesized using the sol-gel method and calcined at various temperatures.

Table 3.2. Crystal lattice parameters of TiO_2 material obtained from the XRD pattern.

Parameter	350°C	450°C	550°C	650°C	750°C	850°C
Crystal Phase	Brookite, Anatase	Brookite, Anatase	Brookite, Anatase, rutile	Anatase, Rutile	Rutie	Rutile
2θ (degree)	25.502	25.502	25.502	27.644	27.644	27.644
FWHM (radian)	1.04	0.811	0.47	0.18	0.17	0.16
Particle size (nm)	15.68	20.1	34.69	90.97	96.32	136.46
(hkl)	101	101	101	110	110	110

3.1.1.2. Photocatalytic activity of TiO_2

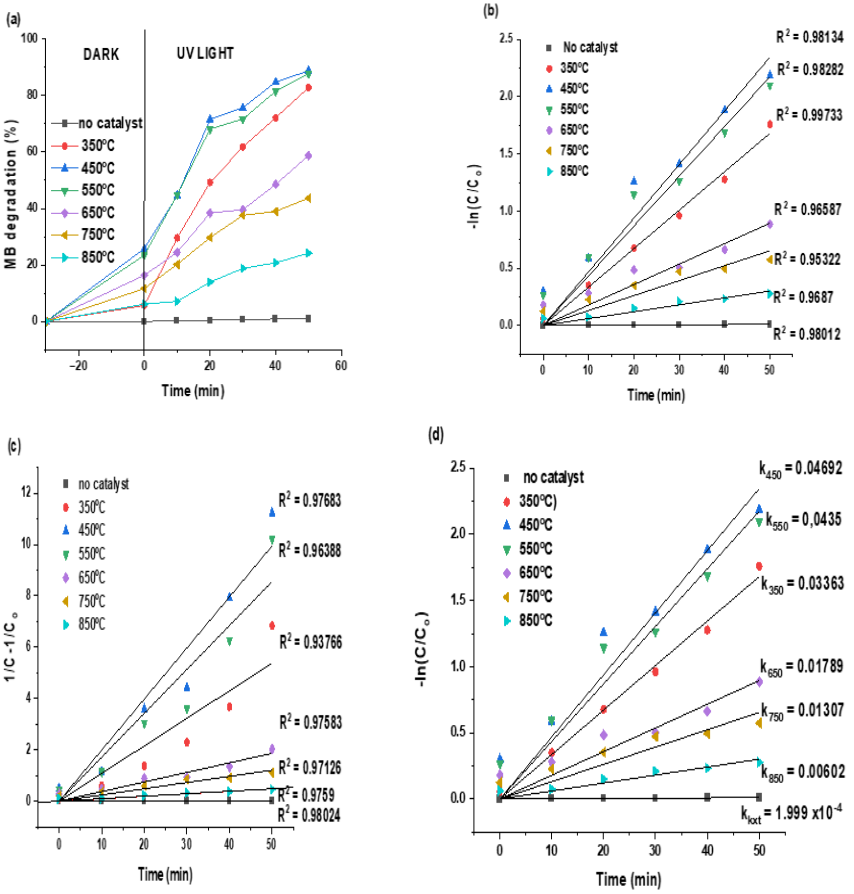

Figure 3.7. (a) Degradation efficiency, (b) first-order kinetic R^2 correlation coefficient, (c) second-order kinetic R^2 correlation coefficient, and (d) reaction rate constant values of the MB degradation process

All synthesized TiO_2 can effectively degrade organic dyes when exposed to UV light. TiO_2 that has been calcined at 450 °C shows the highest photocatalytic activity in the UV region . This material is capable of decomposing methylene blue (MB) and rhodamine B (RhB) with rate constants of k = 0.04692 min^{-1} (for MB) and k = 0.0139 min^{-1} (for RhB),

respectively. The synthesized TiO_2 exhibits greater efficiency in catalyzing the degradation of MB compared to RhB.

3.1.2. Ag modified TiO_2

c) Selected area electron diffraction (SAED) and high-resolution transmission electron microscopy (HRTEM) of Ag modified TiO_2 materials

Silver nanoparticles (Ag) were uniformly distributed on the surface of titanium dioxide (TiO_2). The lattice distance of TiO_2 is 0.35 nm, while that of silver is 0.23 nm.

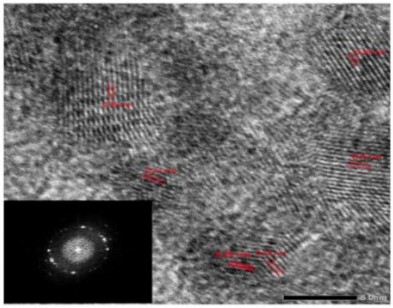

Figure 3.11. HRTEM images at high magnification of Ag/TiO_2

d) X-ray photoelectron spectrum (XPS) of Ag-modified TiO_2 material

The energy difference between the $Ti^{4+}2p_{1/2}$ and $Ti^{4+}2p_{3/2}$ states is 5.75 eV, which is consistent with the standard binding energy of TiO_2. The high-resolution XPS spectra of silver (Ag) show two distinct peaks: Ag $3d_{5/2}$ at 368.4 eV and $Ag3d_{3/2}$ at 374.4 eV. This indicates that silver exists in its metallic form.

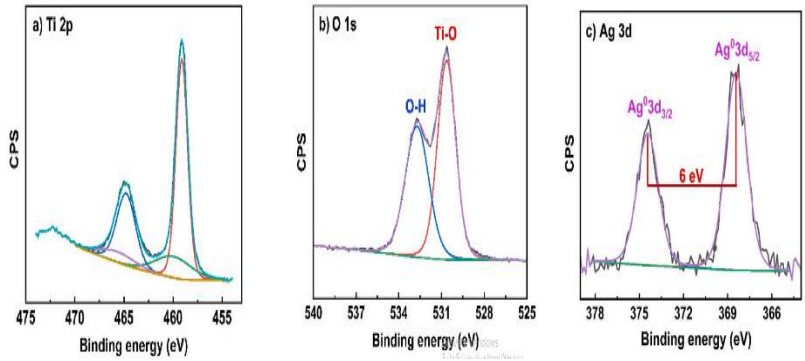

Figure 3.12. High resolution (a) Ti 2p, (b) O 1s and (c) Ag 3d XPS spectra of Ag/TiO_2

e) Photoluminescence spectra (PL) of Ag modified TiO_2

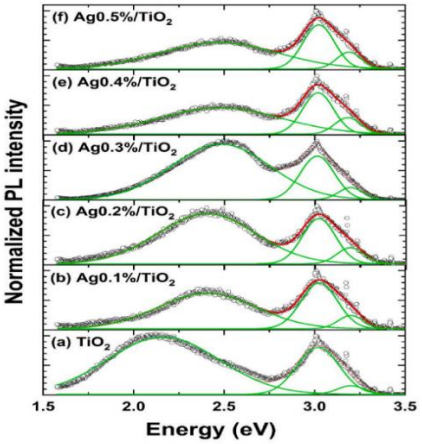

Figure 3.13. PL spectra of (a)TiO_2, (b)Ag0.1%/TiO_2, (c)Ag0.2%/TiO_2, (d)Ag0.3%/TiO_2, (e) Ag0.4%/TiO_2 and (f) Ag0.5%/TiO_2. The open circles and the lines are the experimental observations and the Gaussian fitted emission spectra, respectively

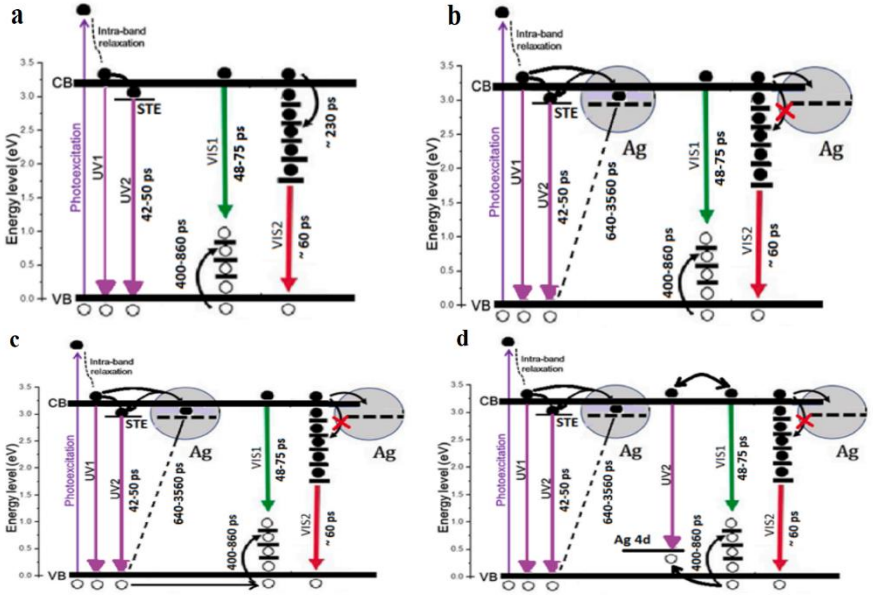

Figure 3.17. Schematic diagram of the decay pathways that are available upon photoexitation to the different populations of (a) TiO_2, (b) Ag0.1%-0.2%/TiO_2, (c) Ag0.3%/TiO_2, (d) Ag0.4 %-0.5% TiO_2

3.1.2.2. Photocatalytic activity of Ag modified TiO_2

TiO_2, when modified with silver (Ag) at weights ranging from 0.1% to 0.5%, exhibits improved photocatalytic efficiency in the UV region compared to pure TiO_2. Among these modifications, the sample with 0.3% Ag/TiO_2 demonstrates the highest photocatalytic efficiency. Consequently, this specific Ag weight content was chosen for further modification processes.

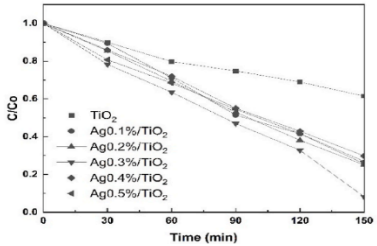

Figure 3.19. MB degradation efficiency of TiO_2 and Ag/TiO_2

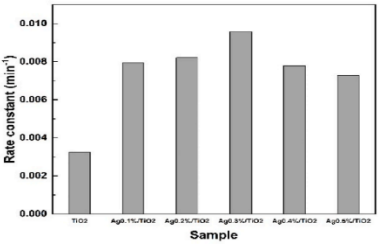

Figure 3.20. Rate constant of MB degradation reaction of TiO_2 and Ag/TiO_2

3.1.3. N-doped graphene quantum dots and silver modified TiO_2

3.1.3.1. Characteristics of N-GQDs modified

a) XRD pattern of N-GQDs modified TiO_2

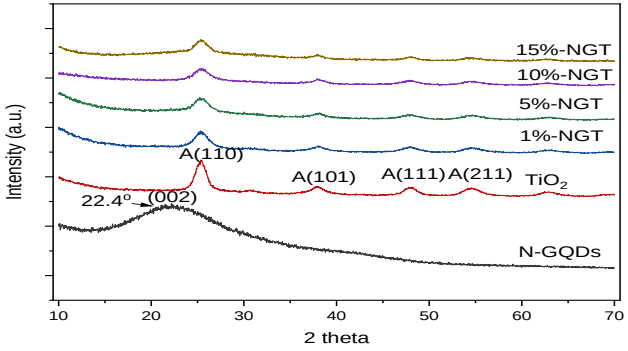

Figure 3.21. XRD pattern of TiO_2 and N-GQDs/TiO_2

c) UV-Vis spectra of N-GQDs modified TiO_2

The band gap energy of TiO_2 decreases when it is combined with N-GQDs materials, resulting in a red shift of the light absorption edge of these hybrid materials toward longer wavelengths. The N-GQDs 5%/TiO_2 composite exhibits the lowest band gap at 3.02 eV.

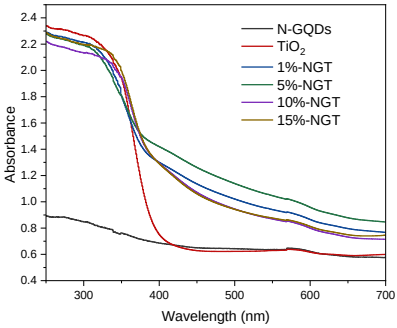

Figure 3.23. UV-Vis spectra of N-GQDs, pure TiO_2 and N-GQDs/TiO_2

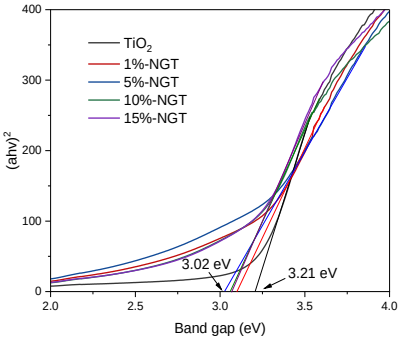

Figure 3.24. Tauc plot and band gap of TiO_2 and N-GQDs/TiO_2

e) High-Resolution Transmission Electron Microscopy of N-GQDs modified TiO_2

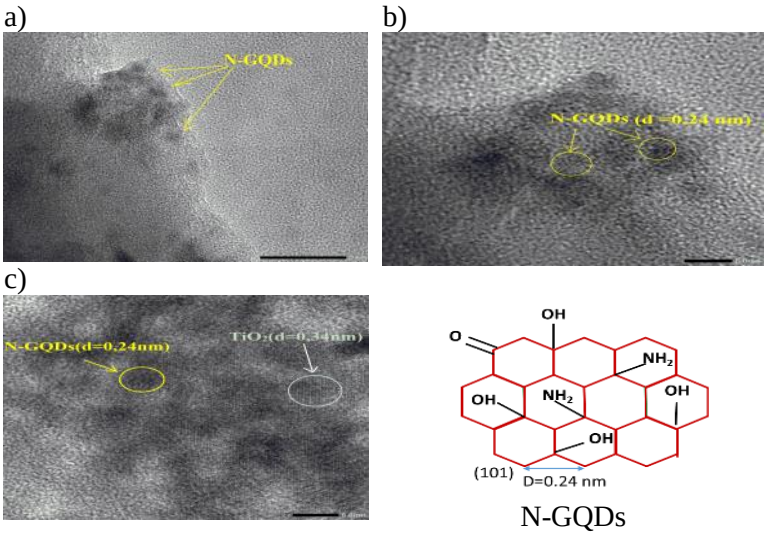

Figure 3.26. HRTEM image of (a) N-GQDs and (b) N-GQDs/TiO_2

f) XPS spectra of N-GQDs modified TiO_2

The blue shift of the Ti 2p peak can be attributed to a decrease in electron density around the titanium nuclei, resulting from a more negatively charged environment. The surface of nitrogen-doped graphene quantum dots (N-GQDs) contains various oxygen functional groups, contributing to this negative charge. Additionally, high-resolution X-ray photoelectron spectroscopy (XPS) of the N 1s region reveals only one signal, which is characteristic of the amine groups (N-H) present in N-GQDs.

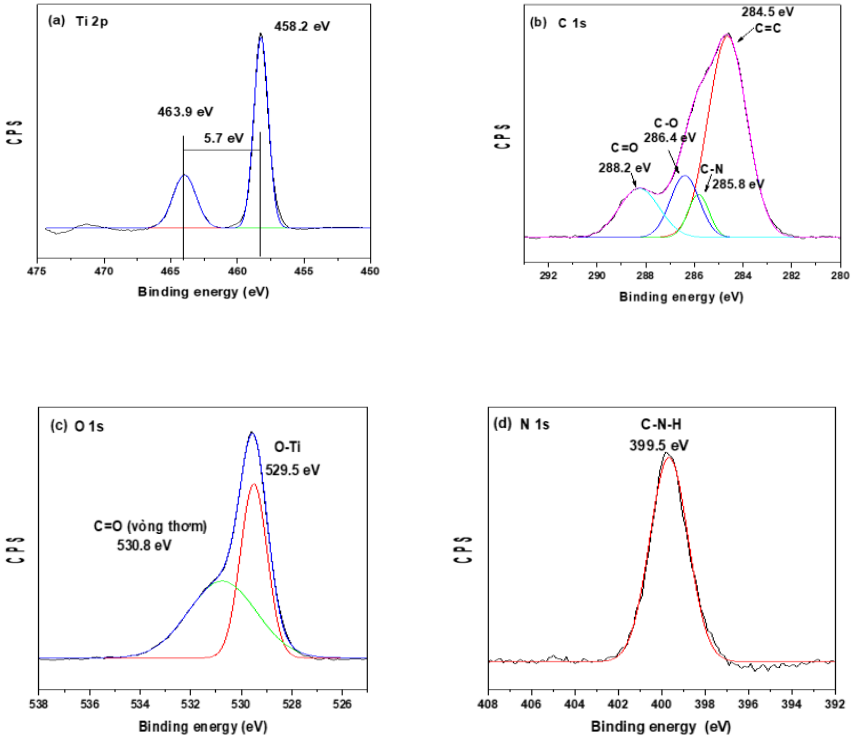

Figure 3.27. XPS spectra (a) Ti 2p, (b) C 1s, (c) O 1s and (d) N 1s of N-GQDs/TiO_2

3.1.3.2. Photocatalytic activity of N-GQDs modified TiO_2

The TiO_2 material adsorbs 35.29% of the MB concentration. The MB adsorption percentages for 1%-NGT, 5%-NGT, 10%-NGT, and 15%-NGT

are higher than those of TiO_2, by 11.7%, 16.69%, 19.84%, and 19.43%, respectively. The adsorption mechanism for the interaction between N-GQDs/TiO_2 and methylene blue is illustrated in Figure 3.30.

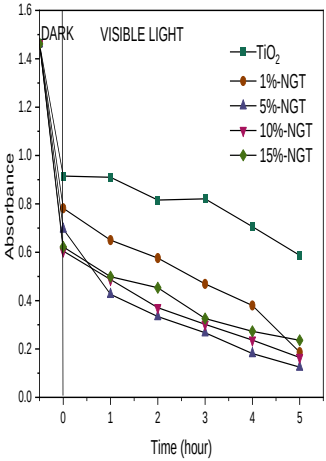

Figure 3.28. The absorbance of MB degradation under white light irradiation of TiO_2 and N-GQDs/TiO_2

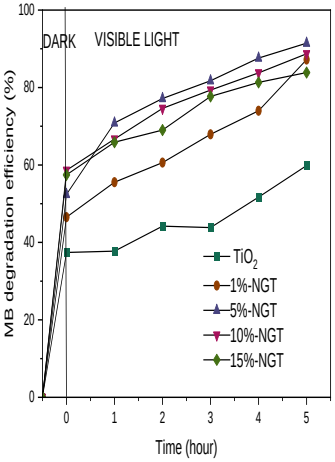

Figure 3.30. The MB decomposition efficiency of TiO_2 and N-GQDs/TiO_2

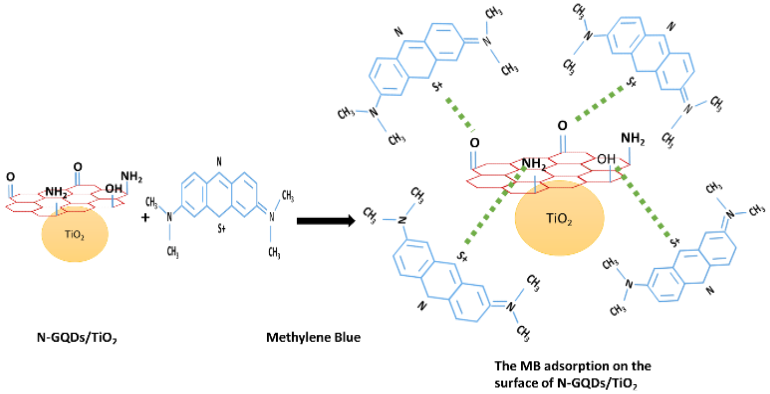

Figure 3.31. The adsorption interaction between N-GQDs/TiO_2 and methylene blue

The photocatalytic properties of pure TiO_2 and TiO_2 modified with nitrogen-doped graphene quantum dots (N-GQDs) in the visible region are better described by second-order kinetics. The 5% N-GQD modified TiO_2

exhibits the highest photocatalytic capacity, with a rate constant of 1.3 L/mol·hour, which is six times higher than that of pristine TiO_2.

3.1.4. Ag, N-GQDs modified TiO_2

3.1.4.1. Characteristics of Ag, N-GQDs/TiO_2

a) XRD pattern of Ag, N-GQDs/TiO_2

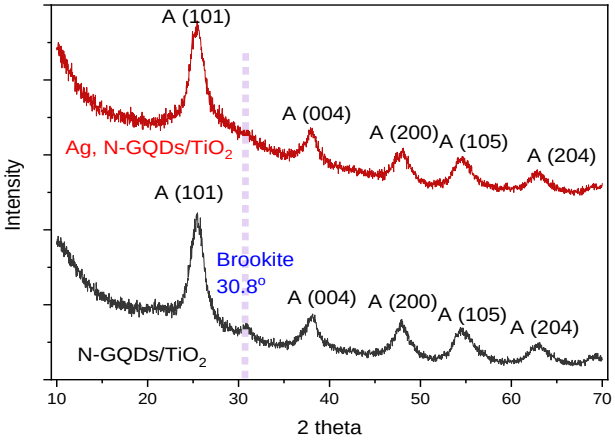

Figure 3.33. XRD pattern of N-GQDs/TiO_2 and Ag, N-GQDs/TiO_2

The size of the crystals can be determined using the Scherrer equation along with the collected data, as illustrated in Table 3.9.

Table 3.9. The crystal sizes of N-GQDs/TiO_2 and Ag, N-GQDs/TiO_2 were analyzed using XRD

Paremeter	N-GQDs/TiO_2	Ag, N-GQDs/TiO_2
Peak (2theta)	25.3	25.3
FWHM (theta)	0.725	0.8
FWHM (radian)	0.012654	0.013963
Crystal size (nm)	11.24	10.19

c) UV – Vis spectra of Ag, N-GQDs/TiO_2

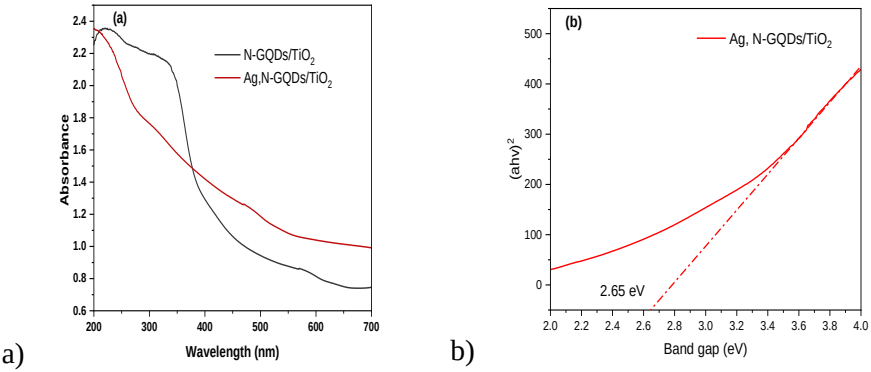

a) b)

Figure 3.35. (a) UV-Vis and (b) Tauc plot of Ag, N-GQDs/TiO₂

f) XPS spectra of Ag, N-GQDs/TiO₂

Figure 3.39. XPS spectra of Ag, N-GQDs/TiO₂

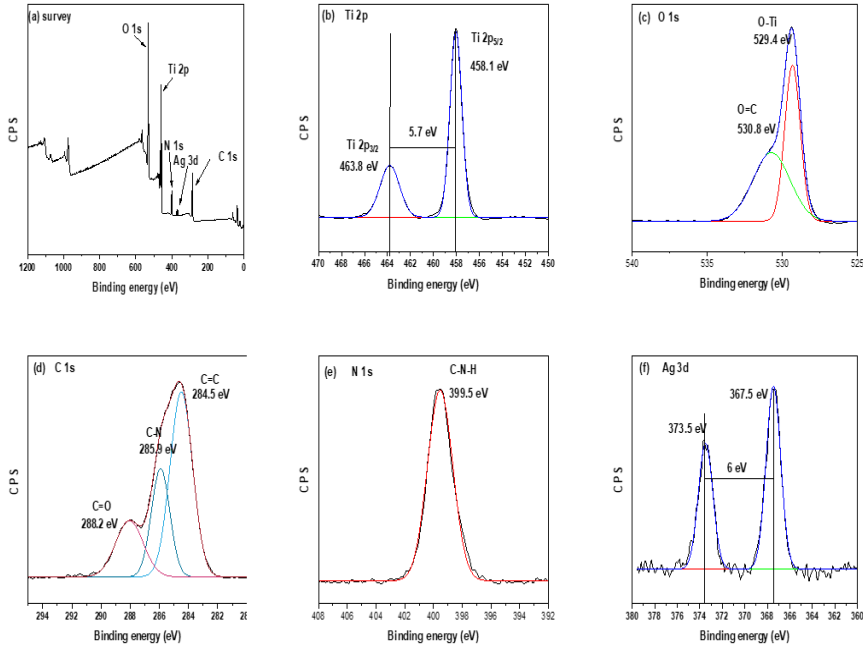

The disappearance of O-H functional groups in the O 1s spectrum, along with the decreased intensity of the C-O peak in the C 1s spectrum,

indicates that C-O-H functional groups may be involved in the reduction process of Ag^+ ions.

3.1.4.2. Photocatalytic activity of Ag, N-GQDs/TiO_2

Regarding the photocatalytic activity of Ag, N-GQDs/TiO_2, the degradation of methylene blue (MB) in the visible region was analyzed. The reaction kinetics for TiO_2, N-GQDs/TiO_2, and Ag, N-GQDs/TiO_2 best fit the pseudo-second-order model. Among these, Ag, N-GQDs/TiO_2 achieved the maximum rate constant (k = 2.1129 L/mol·hour), which is ten times greater than that of pure TiO_2 and three times greater than that of N-GQDs/TiO_2.

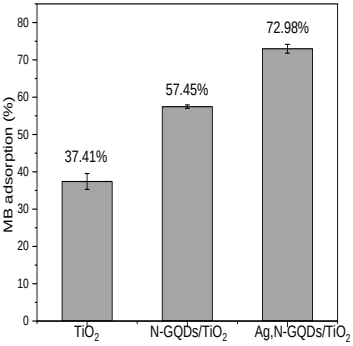

Figure 3.41. The MB absorption yield of TiO_2, N-GQDs/TiO_2, and Ag, N-GQDs/TiO_2

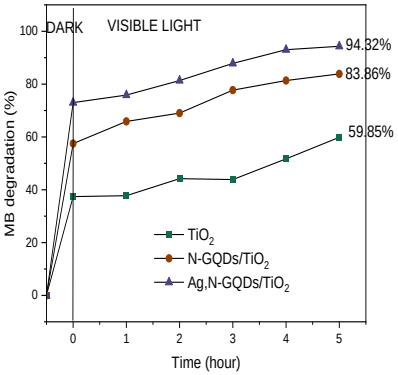

Figure 3.42. The MB degradation efficiency over time of TiO_2, N-GQDs/TiO_2, and Ag, N-GQDs/TiO_2

Table 3.10. The rate constant of the MB degradation reaction under visible light irradiation of TiO_2, N-GQDs/TiO_2, and Ag, N-GQDs/TiO_2

Material	First pseudo-kinetic		Second pseudo-kinetic	
	R^2	k	R^2	k
TiO_2	0.86241	0.1972	0.90279	0.20232
N-GQDs/TiO_2	0.88021	0.43184	0.9615	0.74909
Ag,N-GQDs/TiO_2	0.90032	0.65616	0.96834	2.1129

3.2. Research results on the characteristics and photocatalytic activity of Ag, N-GQDs/ZnO

3.2.1. Zinc Oxide

3.2.1.1. Characteristics of ZnO

a) XRD of ZnO

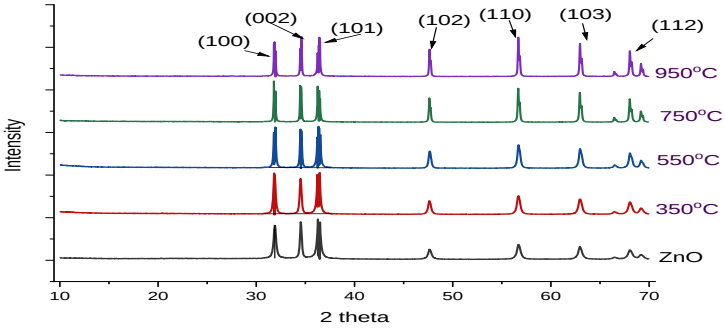

Figure 3.44. XRD pattern of ZnO

The wurtzite structure is the preferred formation of ZnO, which is synthesized using the sol-gel method with water as the solvent at room temperature or when calcined at temperatures below 950 °C under atmospheric pressure. Additionally, the crystal lattice size of ZnO produced by this method is minimally influenced by temperature changes.

3.2.1.2. Photocatalytic activity of ZnO

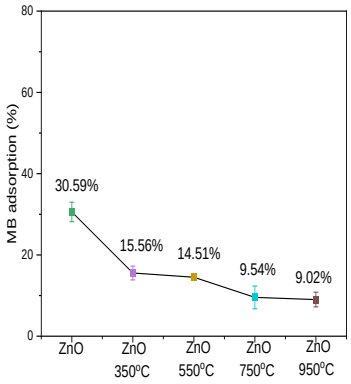

Figure 3.52. The MB adsorption efficiency of ZnO

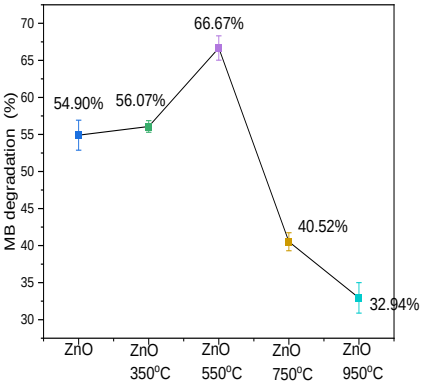

Figure 3.53. The MB degradation yield of ZnO after 50 mins UV irradiation

The MB degradation process under UV light is better described by the first pseudo kinetic model (2.11). The ZnO calcined at 550 °C demonstrates the best capability for MB degradation ($k = 0.01696\ min^{-1}$).

3.2.2. Ag modified ZnO

3.2.2.1. Characteristics of ZnO

d) EDX spectra of Ag modified ZnO

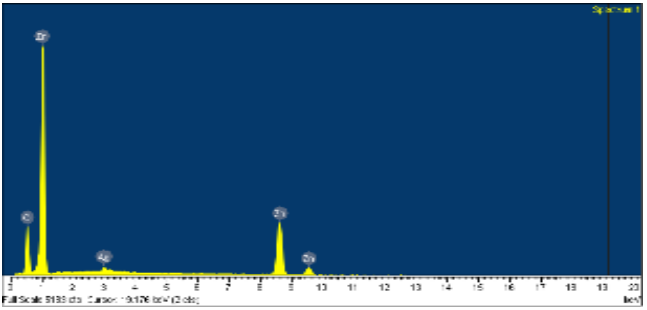

Figure 3.59. EDX spectra of Ag1%/ZnO

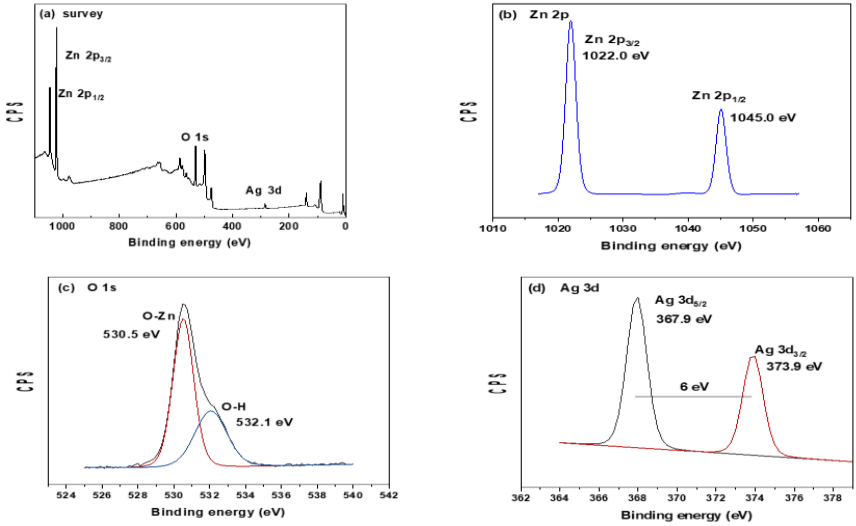

Figure 3.60. XPS spectra of Ag1%/ZnO (a) survey, (b) Zn 2p. (c) O 1s, and (d) Ag 3d

e) XPS spectra of Ag modified ZnO

The XPS survey shown in Figure 3.60a reveals signals for Zn 2p, O 1s, and Ag 3d. The high-resolution XPS spectra for Ag 3d (Figure 3.60d) display two distinct peaks at 367.9 eV and 393.9 eV, which correspond to the Ag $3d_{5/2}$ and Ag $3d_{3/2}$ levels, respectively. The binding energy difference between these peaks remains consistent at 6 eV. Notably, there is no additional peak for Ag^{+}, indicating that silver is present in its metallic form.

3.2.2.2. Photocatalytic activity of Ag modified ZnO

a. Photocatalytic activity of Ag/ZnO for MB degradation

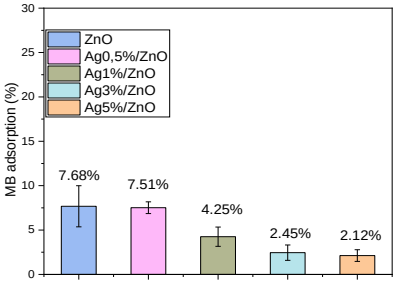

Figure 3.62. The MB adsorption efficiency after 30 minutes in the dark

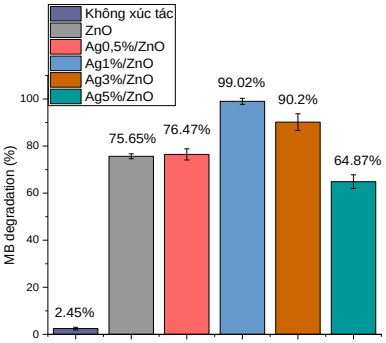

Figure 3.63. The MB degradation efficiency after 50 minutes under UV irradiation

b. Photocatalytic activity of Ag/ZnO for caffeine degradation

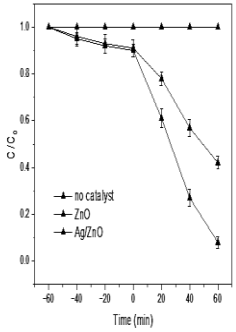

Figure 3.64. Photodegradation of caffeine using different catalysts

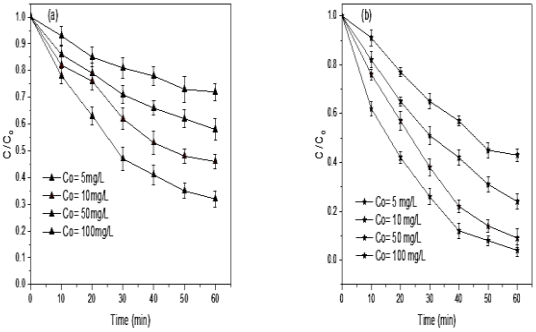

Figure 3.65. Effect of initial concentration on degradation of caffeine using (a) ZnO và (b) Ag/ZnO

The proposed mechanism of caffeine degradation using Ag/ZnO catalyst under sunlight irradiation is as follows:

$$Ag/ZnO + hv \rightarrow Ag/ZnO\ (e^- + h^+)$$

$$e^- + O_2 \rightarrow O_2^{\bullet -}$$

$$h^+ + H_2O \rightarrow OH^\bullet + H^+$$

$$OH^\bullet, O_2^{\bullet -} + \text{caffeine} \rightarrow H_2O + CO_2 + \text{by products}$$

The stability of the Ag/ZnO photocatalyst was evaluated over eight testing cycles. The Ag/ZnO demonstrated a remarkable photodegradation capacity for caffeine, achieving 78.6% degradation after five cycles. However, this effectiveness declined to 48.2% by the eighth cycle.

3.2.3. Ag, N-GQDs/ZnO

3.2.3.1. Characteristics of Ag, N-GQDs/ZnO

c) SEM image of Ag, N-GQDs/ZnO

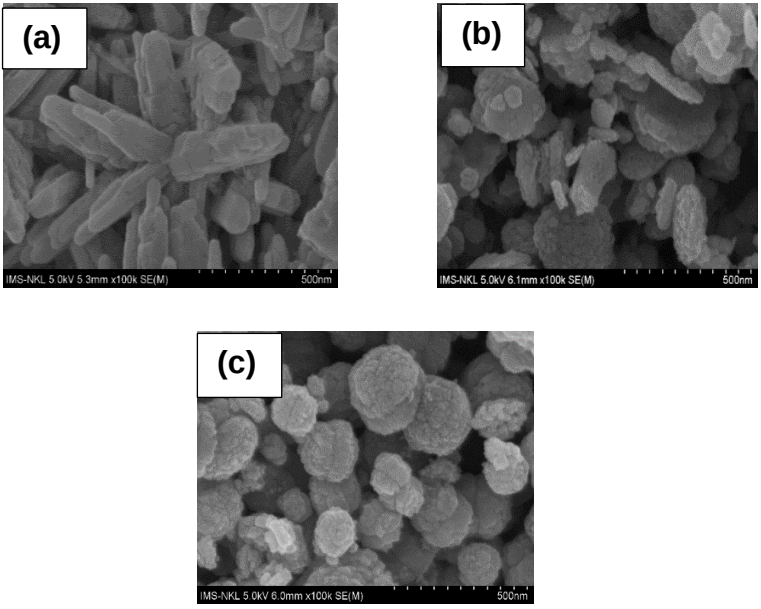

Figure 3.71. SEM image of (a) ZnO, (b) N-GQDs/ZnO, (c) Ag, N-GQDs/ZnO

The N-GQDs dots act as a capping agent that will change the shape of the forming material. The N-GQDs/ZnO material has a plate-like structure, with a nanometer thickness of about 25 nm - 50 nm.

d) UV-Vis spectra of Ag, N-GQDs/ZnO

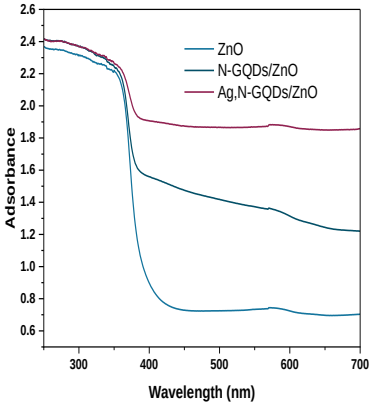

Figure 3.72. UV-Vis spectra of ZnO, N-GQDs/ZnO, and Ag, N-GQDs/ZnO

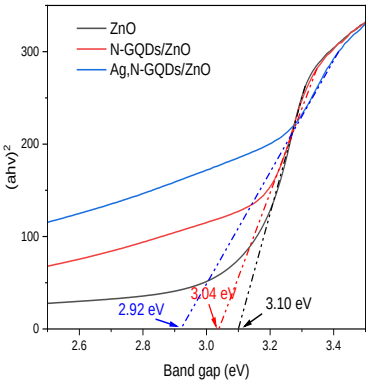

Figure 3.73. Tauc plot and band gap of ZnO, N-GQDs/ZnO, and Ag, N-GQDs/ZnO

The band gap energies for ZnO, N-GQDs/ZnO, and Ag, N-GQDs/ZnO are 3.10 eV, 3.04 eV, and 2.92 eV, respectively (Figure 3.73). The simultaneous combination of noble metal and carbon nanomaterials with ZnO can reduce the band gap energy to a level lower than that of pure ZnO and the N-GQDs/ZnO hybrid material.

d) Energy dispersive X-ray spectrum of Ag, N-GQDs/ZnO materials

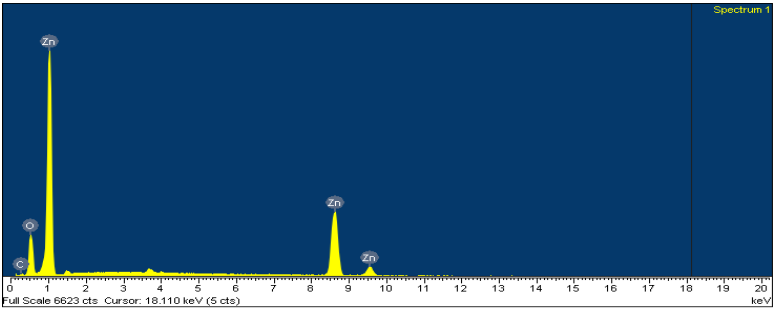

Figure 3.74. EDX image of N-GQDs/ZnO

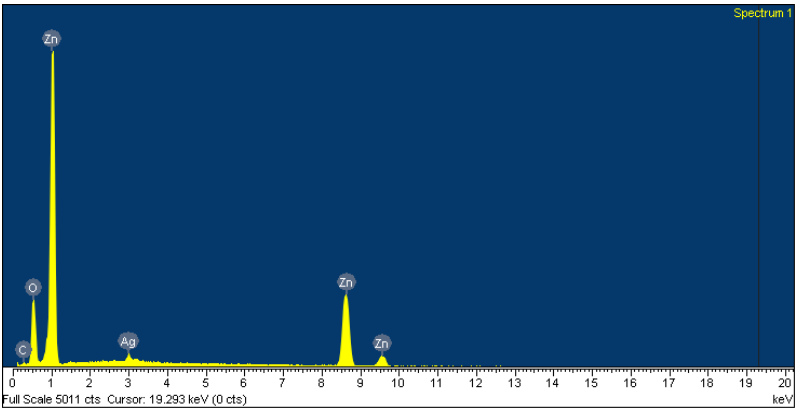

Figure 3.75. EDX image of Ag, N-GQDs/ZnO

3.2.3.2. Photocatalytic activity of Ag, N-GQDs/ZnO

Table 3.20. Rate constant values of the MB degradation reaction under visible light of ZnO, N-GQDs/ZnO, and Ag, N-GQDs/ZnO

Material	First pseudo-kinetic		Second pseudo-kinetic	
	Coefficient R^2	Rate constant - k ($hour^{-1}$)	Coefficient R^2	Rate constant - k (L/mol.hour)
ZnO	0.8229	0.12314	0.84694	0.20436
N-GQDs/ZnO	0.79864	0.20415	0.83689	0.39996
Ag, N-GQDs/ZnO	0.76903	0.20415	0.81386	0.69519

Modifying ZnO with graphene quantum dots (N-GQDs) and noble metal nanoparticles like silver (Ag) will enhance the photocatalytic capability of this material in the visible region by up to 3.5 times.

CONCLUSION

During the research and development of photocatalytic materials based on TiO_2 and ZnO, which were modified with nitrogen-doped graphene quantum dots and Ag nanoparticles, the following results were obtained:

1. The materials TiO_2 and ZnO were successfully fabricated using the sol-gel method, followed by high-temperature calcination. TiO_2 undergoes a phase transformation, with the rutile phase emerging at calcination

temperatures above 650 °C. All the fabricated TiO_2 materials are capable of decomposing organic dyes when exposed to ultraviolet (UV) light. Specifically, the TiO_2 material calcined at 450 °C exhibits the highest effectiveness in decomposing methylene blue (MB) and rhodamine B (RhB) in the UV range, achieving decomposition rates of 88.76% and 50.05%, respectively. This material has a mixed structure, consisting of approximately 88.6% anatase and 11.34% brookite, with a spherical shape and an average size of about 20 nm. Conversely, the ZnO material calcined at 550 °C demonstrates the highest efficiency in decomposing MB under UV light, achieving a decomposition rate of 66.67%. This ZnO possesses a wurtzite crystal structure, a spherical shape, and a low bandgap energy of approximately 3.06 eV. On the other hand, the uncalcined ZnO material features a long rod shape but shares the same bandgap energy of 3.06 eV. It exhibits a superior ability to absorb visible light, making it advantageous for photocatalysis in the visible range.

2. Silver-modified TiO_2 and ZnO were fabricated using a chemical reduction method combined with UV irradiation. The Ag/TiO_2 materials, with silver content ranging from 0.1% to 0.5%, demonstrated a superior ability to decompose methylene blue (MB) in the UV region compared to pure TiO_2. Silver acts as an electron trap, which increases the average lifetime of the electron-hole pairs from 42.12 ps to 77.51 ns. For ZnO surface modification, the optimal silver content was found to be 1%, resulting in a band gap energy of 2.93 eV. The Ag/ZnO material was able to decompose 99.02% of MB under UV light and 97.20% of caffeine using sunlight. After five reuse cycles, Ag/ZnO decomposed 78.6% of caffeine, with superoxide ($O_2^{\bullet-}$) identified as the primary agent responsible for caffeine decomposition in aqueous environments.

3. A simple mixing method was successfully used to fabricate N-GQDs/TiO_2 and N-GQDs/ZnO materials. The N-GQDs (nitrogen-doped graphene quantum dots) measured approximately 5 nm in size and featured oxygen-containing functional groups on their surfaces, which enhanced their ability to adsorb methylene blue (MB). In the visible region, the N-GQDs/TiO_2 composite with 5% N-GQDs decomposed MB at a rate twice

that of TiO_2 alone, achieving a reaction rate constant of 1.29838 l/mol·hour. The MB decomposition reaction rate constant for the N-GQDs/ZnO material is 0.39996 l/mol·hour. Additionally, the band gap energy of N-GQDs/TiO_2 is 3.02 eV, while that of N-GQDs/ZnO is 3.04 eV.

4. Multilayer Ag, N-GQDs/TiO_2 and Ag, N-GQDs/ZnO materials were successfully fabricated using a chemical reduction method. The hydroxyl (OH) functional groups on the surface of N-GQDs serve as direct agents that reduce Ag^+ ions into Ag nanoparticles. The band gap energies of the Ag, N-GQDs/TiO_2 and Ag, N-GQDs/ZnO materials are measured at 2.65 eV and 2.92 eV, respectively. These materials demonstrate visible light decomposition efficiencies for methylene blue (MB) of 94.23% and 68.37%. The decomposition reaction rate constants for Ag, N-GQDs/TiO_2 and Ag, N-GQDs/ZnO materials are 2.1129 L/mol.hour and 0.69519 L/mol.hour, respectively.

RECOMENDATION

The thesis has presented a scientific foundation and the synthesis process for a new generation of photocatalytic materials that function efficiently in the visible light spectrum. This is achieved by combining traditional TiO_2 and ZnO with precious metal nanoparticles, specifically silver (Ag), and nitrogen-doped graphene quantum dots. The research findings indicate that these new materials demonstrate a superior ability to photodegrade organic compounds in the visible region. This capability allows them to replace catalysts that only work under UV light, thus optimizing the utilization of natural sunlight to treat dissolved pollutants in water. However, due to time and resource constraints during the thesis implementation, it is recommended to continue exploring the following areas:

It is essential to continue studying the visible light photocatalytic abilities of Ag, N-GQDs/TiO_2, and Ag, N-GQDs/ZnO materials in real wastewater. Additionally, we need to evaluate the factors that affect the photocatalytic performance of these materials.

Furthermore, it is important to design an optimized reactor system to enhance the wastewater treatment process using Ag, N-GQDs/TiO_2 and Ag, N-GQDs/ZnO photocatalytic materials.

LIST OF THE PUBLICATIONS RELATED TO THE DISSERTATION

1. Minh Thuy Pham, Thi Thu Hien Chu, Duc Chinh Vu, "Mitigation of caffeine micropollutants in wastewater through Ag-doped ZnO photocatalyst: mechanism and environmental impacts", Environ Geochem Health (2024) 46:168
https://doi.org//s10653-024-01952-1

2. Minh Thuy Pham, Duc Chinh Vu, Thi Thu Hien Chu, Thuy Van Nguyen, "Multi-timescale map of radiative and nonradiative decay for exciton in Ag/TiO_2 nanoparticles" Optical Materials /159 (2025) 116607
https://doi.org/10.1016/j.optmat.2024.116607